JOURNAL OF MATERIALS SCIENCE **20** (1985) 4057–4068

Enthalpy relaxation behaviour of metal–metal (Zr–Cu) amorphous alloys upon annealing

A. INOUE*[‡], T. MASUMOTO[§], H. S. CHEN[‡]
[‡]*AT&T Bell Laboratories, Murray Hill, New Jersey 07974, USA and*
[§]*The Research Institute for Iron, Steel and Other Metals, Tohoku University, Sendai 980, Japan*

Anneal-induced enthalpy relaxation behaviour was examined calorimetrically for $Zr_{50-70}Cu_{50-30}$, $Zr_{70}(Cu–Fe)_{30}$ and $Zr_{70}(Cu–Ni)_{30}$ amorphous alloys. When the alloys annealed at temperatures below T_g are heated, an excess endothermic reaction (enthalpy relaxation) occurs above the annealing temperature T_a. The peak temperature of $\Delta C_{p,endo}$, evolves in a continuous manner with $\ln t_a$. The magnitudes of $\Delta C_{p,endo}$ and ΔH_{endo} for Zr–Cu binary alloys increase gradually with rising T_a and then rapidly at temperatures just below T_g, while their changes as a function of T_a for the ternary alloys show a distinct two-stage splitting; a low-temperature one which peaks at about $T_g - 150$ K and a high-temperature peak just below T_g. From the result that the addition of iron or nickel causes the two stage splitting of the $\Delta C_{p,endo}$ (T_a), it was proposed that the low-temperature endothermic peak is attributed to local and medium range rearrangments of copper and iron or nickel atoms with weak bonding nature and the high-temperature reaction to the long-range co-operative regroupings of zirconium and copper, iron or nickel atoms which are composed of the skeleton structure in the metal–metal amorphous alloys. The mechanism for the appearance of the two-stage enthalpy relaxation was investigated by the concept of two-stage distributions of relaxation times proposed previously, and the distinct two-stage splitting was interpreted as arising from the distinctly distinguishable difference in the ease of atomic rearrangements between Cu–(Fe or Ni) and Zr–(Cu, Fe or Ni).

1. Introduction

Recently, it has been found for a number of metal–metalloid amorphous alloys such as Fe–Ni–P–B–Al [1–3], Pd–Ni–(P or Si) [4, 5] and (Fe, Co, Ni)–Si–B [6] that the amorphous alloys annealed at temperatures well below glass transition temperature (T_g) or crystallization temperature (T_x) exhibit a reversible endothermic peak at a temperature slightly higher than the annealing temperature (T_a), and that further heating results in the same irreversible exothermic reaction as that of the as-quenched sample. Most recently, the reversible endothermic reaction as a function of T_a was found to occur in two stages in metal–metalloid amorphous alloys containing more than two kinds of metal elements such as (Fe, Co, Ni)–Si–B [6], Fe–Ni–P [7] and Fe–Ni–B [7] systems and it was concluded [7] that the low-temperature endothermic reaction is attributed to local and medium-range rearrangements of metal atoms, and the high-temperature reaction to long-range co-operative regroupings of metal and metalloid atoms. Furthermore, the mechanism for the

Permanent address: The Research Institute for Iron, Steel and Other Metals, Tohoku University, Sendai 980, Japan.

appearance of the two-stage enthalpy relaxation was interpreted based on the new concept of two-stage distribution in relaxation times (e.g. two-stage glass transitions).

The concept of the distribution of the glass transition due to metal–metal atoms with shorter relaxation times is quite significant in the understanding of the thermal stability of various kinds of properties for metal–metalloid type amorphous alloys annealed at temperatures well below T_g and/or T_x, because the relaxation due to the interaction of metal–metal atoms is faster by many orders of magnitude than the co-operative relaxation process due to metal–metalloid atoms responsible for the commonly observed glass transition. Thus, a lot of useful information has been obtained on the structural relaxation behaviour of metal–metalloid type amorphous alloys. However, there is no quantitative information available on the reversible endothermic reaction for metal–metal type amorphous alloys, even though a trial to clarify the anneal-induced relaxation behaviour has been actively made for Cu–Zr [8, 9], Cu–Ti [9] and Zr–Ni [9] alloys. The purpose of the present investigation is threefold; (a) to clarify quantitatively the T_a and t_a dependences of the anneal-induced structural relaxation behaviour, especially the enthalpy relaxation behaviour, for amorphous $Zr_{100-x}Cu_x$ binary and $Zr_{70}(Cu-Fe)_{30}$ and $Zr_{70}(Cu-Ni)_{30}$ ternary alloys; (b) to ascertain whether or not the two-stage enthalpy relaxation behaviour, which was first found for the metal–metalloid amorphous alloys of (Fe, Co, Ni)–Si–B, Fe–Ni–P and Fe–Ni–B etc., is observed even for the present metal–metal amorphous alloys; and (c) to clarify the copper concentration dependence of the enthalpy relaxation behaviour of Zr–Cu binary alloys including eutectic and compound compositions.

2. Experimental methods

Ribbon samples of $Zr_{70}Cu_{30}$, $Zr_{67}Cu_{33}$, $Zr_{55}Cu_{45}$ and $Zr_{50}Cu_{50}$ binary and $Zr_{70}(Cu_{1-x}Fe_x)_{30}$ and $Zr_{70}(Cu_{1-x}Ni_x)_{30}$ ($x = 0.25, 0.50, 0.75$) ternary alloys, typically 20 μm in thickness and 1 mm in width, were prepared in argon atmosphere by a single-roller melt spinning method and confirmed to be amorphous by a conventional X-ray diffractometer using Cu$K\alpha$ radiation in combination with an X-ray monochrometer. The subscripts are assumed to be those of the unalloyed pure elements, since the difference between nominal and chemically analysed compositions was less than 0.3 wt % for copper and iron and 0.25 wt % for nickel. The apparent specific heat C_p was measured with a differential scanning calorimeter (Perkin Elmer DSC–II). Care was taken to reduce the thermal drift by prewarming the calorimeter for at least 5 h in the temperature range of interest. The accuracy of the data was about 0.8 J mol^{-1} K^{-1} for the absolute C_p values, but was better than 0.2 J mol^{-1} K^{-1} for the relative C_p and ΔC_p measurements.

The as-quenched samples were subjected to annealing treatments at various temperatures below T_g (T_a = 373 to 593 K for different periods (t_a = 1 to 100 h). Short-period anneals ($t_a \leqslant 3$ h) were performed directly inside the calorimeter while long-time anneals (4 to 100 h) were performed in a well-controlled furnace after placing the encapsulated samples in a vacuum-sealed quartz tube.

Following the annealing treatment, the sample was thermally scanned at 40 K min^{-1} from 320 K to T_g to determine the $C_{p,q}$ of the as-quenched or the $C_{p,a}$ of the annealed sample. It was then cooled to 320 K, and reheated immediately to obtain the $C_{p,s}$ data of the "reference" sample (i.e. the preconditioned sample without further low-temperature annealing.) This test procedure is essential in order to eliminate any possible error that might result from the drift in the calorimeter. The change in the calorimetric behaviour with annealing was used in monitoring the structural relaxation processes.

3. Results

3.1. $C_p(T)$ and $\Delta C_p(T)$ behaviour of as-quenched samples

Fig. 1 shows the thermograms of an amorphous $Zr_{55}Cu_{45}$ alloy corresponding to a eutectic composition in the as-quenched state. The C_p value of the as-quenched phase is about 26 J mol^{-1} K^{-1} near room temperature. As the temperature rises, the C_p value begins to decrease indicative of a structural relaxation at about 375 K, exhibits a minimum peak at about 580 K in the range below 650 K, then increases rapidly in the region of glass transition and reaches an equilibrium liquid value of about 45 J mol^{-1} K^{-1} around 700 K. It can be seen that

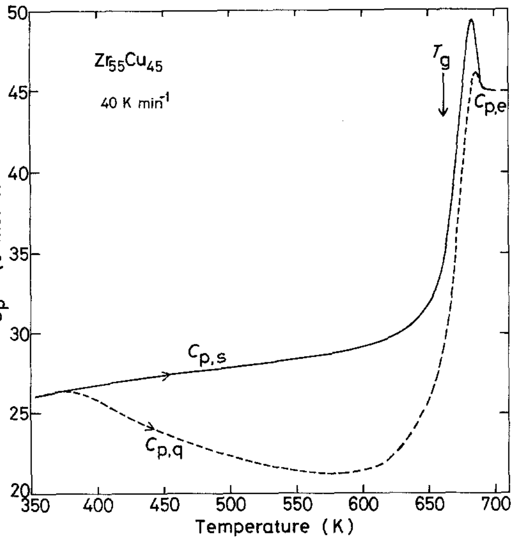

Figure 1 The thermogram of an amorphous $Zr_{55}Cu_{45}$ alloy in the as-quenched state. The solid line presents the thermogram of the sample subjected to heating to 700 K.

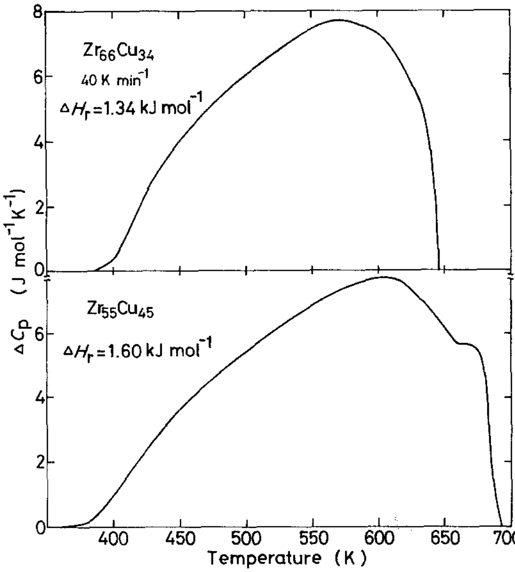

Figure 3 Difference in the specific heat between the as-quenched and annealed states ($\Delta C_{p,exo}$) against temperature for amorphous $Zr_{55}Cu_{45}$ and $Zr_{67}Cu_{33}$ alloys.

the C_p value near room temperature is consistently higher by about 0.1 to 0.2 $J\,mol^{-1}\,K^{-1}$ for the as-quenched sample than for the annealed one. The small difference in C_p is attributed to the anneal-induced changes in physical and mechanical properties. Furthermore, the difference in C_p between amorphous solid and supercooled liquid is estimated to be about 16 $J\,mol^{-1}\,K^{-1}$. Similar thermograms have been obtained for an amorphous $Zr_{67}Cu_{33}$ alloy corresponding to a stoichiometric compound (Zr_2Cu) as shown in Fig. 2. From the comparison of the $C_p(T)$ curves between $Zr_{55}Cu_{45}$ eutectic and $Zr_{67}Cu_{33}$ compound alloys, one can notice the following three differences: (a) the temperature at which the exothermic reaction corresponding to an irreversible structrual relaxation begins to occur is higher by about 15 K for $Zr_{67}Cu_{33}$ than for $Zr_{55}Cu_{45}$ while T_g is lower by about 35 K for $Zr_{67}Cu_{33}$, indicating that the distribution of relaxation entity as a function of temperature is considerably narrower for the Zr_2Cu compound alloy; (b) no distinct supercooled liquid region is recognized for $Zr_{67}Cu_{33}$; and (c) the difference in C_p between supercooled liquid and amorphous solid is smaller by about 14% for $Zr_{67}Cu_{33}$ than for $Zr_{55}Cu_{45}$.

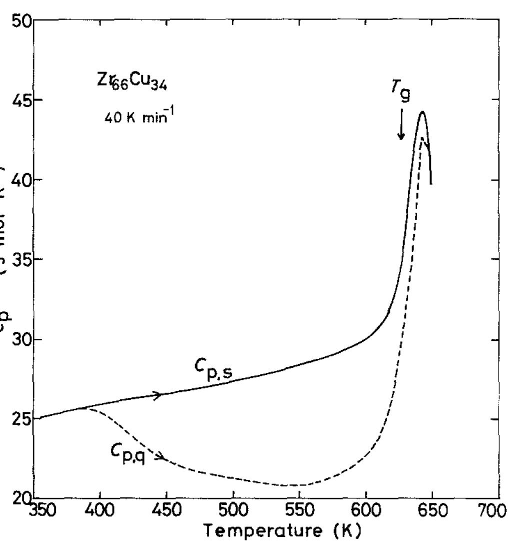

Figure 2 The thermogram of an amorphous $Zr_{67}Cu_{33}$ alloy in the as-quenced state. The solid line presents the thermogram of the sample subjected to heating to 650 K.

Fig. 3 shows the temperature dependence of the difference in C_p between the as-quenched and the annealed states, $\Delta C_p(T)$, for the amorphous $Zr_{55}Cu_{45}$ and $Zr_{67}Cu_{33}$ alloys. Only one broad irreversible relaxation peak with a long tail on the low-temperature side can be seen, and the existence of two separable peaks is not recognized for both alloys, in good contrast to the previous results for the metal–metalloid type amorphous alloys such as (Fe, Ni)–(P or B) [7] and (Fe, Co, Ni)–Si–B [6]. The value of the exothermic relaxation enthalpy change

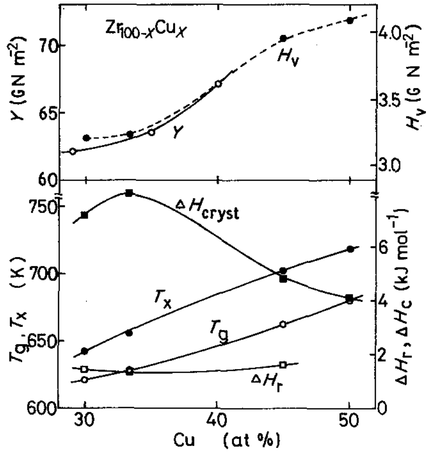

Figure 4 Changes in glass transition temperature T_g, crystallization temperature T_x, exothermic relaxation enthalpy ΔH_r and heat content of crystallization ΔH_c of Zr–Cu amorphous alloys as a function of copper concentration. The data for Vickers hardness H_v and Young's modulus Y are also presented for comparison.

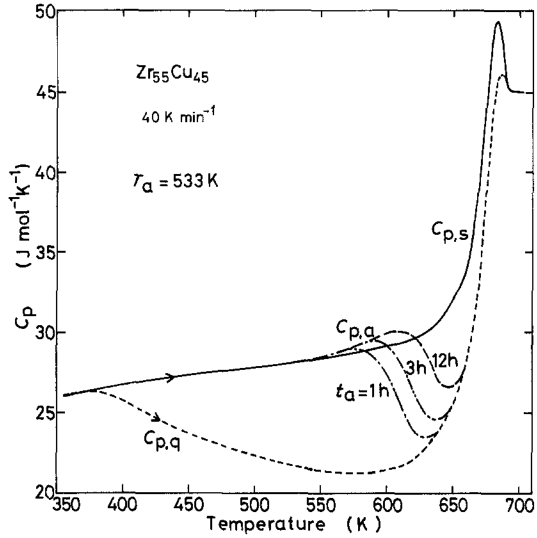

Figure 5 The thermograms of an amorphous $Zr_{55}Cu_{45}$ alloy subjected to anneals at 533 K for various periods from 1 to 2 h. The solid line presents the thermogram of the sample subjected to heating at 700 K.

$\Delta H_r = \int \Delta C_p dT = \int (C_{p,a} - C_{p,q}) dT$ (where subscript q refers to quenching) for $Zr_{55}Cu_{45}$ (1.60 kJ mol^{-1}) is larger by about 16% than that for $Zr_{67}Cu_{33}$ (1.34 kJ mol^{-1}), indicating that the amorphous structure in the Zr_2Cu alloys with a stoichiometric compound composition possesses a more relaxed and stable atomic configuration even in the as-quenched state.

The ΔH_r, T_g and T_x, for Zr–Cu binary amorphous alloys as a function of copper content are shown in Fig. 4, where the heat of crystallization ΔH_{cryst}, the Young's modulus Y and Vickers hardness H_v are also presented for comparison. The features of this figure are described as follows: (a) T_g, T_x, Y and H_v increase monotonically with increasing copper content; (b) ΔH_{exo} shows a minimum value at 33 at % Cu, whereas ΔH_{cryst} exhibits an inverse tendency showing a maximum value at 33 at % Cu. These results enable us to infer that the Zr_2Cu compound alloy has a more relaxed atomic configuration but a higher instability against the completion of crystallization as compared with $Zr_{55}Cu_{45}$ and $Zr_{70}Cu_{30}$ eutectic alloys, even though the difference in atomic configuration hardly reflects on the mechanical properties of Y and H_v as well as the onset temperatures of glass transition and crystallization. The monotonic rise of T_g, T_x, and Y with increasing copper content is in good agreement with the previous data reported by Chen and Krause [10].

3.2. $C_p(T)$ and $\Delta C_p(T)$ behaviour of annealed samples

The change in the $C_p(T)$ behaviour with annealing was examined for $Zr_{50}Cu_{50}$, $Zr_{55}Cu_{45}$, $Zr_{67}Cu_{33}$ and $Zr_{70}Cu_{30}$ amorphous alloys. As an example, Fig. 5 shows the thermograms of an amorphous $Zr_{55}Cu_{45}$ alloy annealed at 533 K for different periods, together with the data of the as-quenched sample. The heating curve of the annealed sample $C_{p,a}$ shows a $C_p(T)$ behaviour which closely follows the specific curve of the reference sample $C_{p,s}$ up to each T_a, and then exhibits an excess endothermic peak relative to the reference sample before merging with that of the as-quenched sample at a temperature below T_g, where T_g is defined as the point of inflection in the $C_p(T)$ curve.

The significant features of Fig. 5 may be summarized as follows:

1. The sample annealed at T_a shows an excess endothermic reaction beginning at T_a, implying that the $C_{p,a}$ curve in the temperature range above T_a is dependent on the thermal history and consists of configurational contributions as well as those arising from purely thermal vibrations. Therefore, the vibrational specific heat $C_{p,v}$ must be extrapolated from C_p values in the low-temperature regions $T \leqslant 530$ K and is a

linear function of temperature such that

$$C_{p,v} = 27.9 + 7.0 \times 10^{-3}(T - 530)\,\mathrm{J\,mol^{-1}\,K^{-1}} \quad (1)$$

Further, the equilibrium specific heat $C_{p,e}$ of the supercooled liquid including the vibrational and configurational specific heat was determined from Fig. 5 as expressed by Equation 2:

$$C_{p,e} = 45.0 + 8.2 \times 10^{-3}(700 - T)\,\mathrm{J\,mol^{-1}\,K^{-1}} \quad (2)$$

Similarly, the $C_{p,v}$ and $C_{p,e}$ of $Zr_{50}Cu_{50}$ and the $C_{p,v}$ of $Zr_{67}Cu_{33}$ and $Zr_{70}Cu_{30}$ were found to be expressed as follows:

$Zr_{50}Cu_{50}$:

$$C_{p,v} = 27.4 + 1.2 \times 10^{-2}(T - 500)\,\mathrm{J\,mol^{-1}\,K^{-1}} \quad (3)$$

$Zr_{50}Cu_{50}$:

$$C_{p,e} = 46.5 + 7.7 \times 10^{-3}(720 - T)\,\mathrm{J\,mol^{-1}\,K^{-1}} \quad (4)$$

$Zr_{67}Cu_{33}$:

$$C_{p,v} = 27.4 + 1.4 \times 10^{-2}(T - 480)\,\mathrm{J\,mol^{-1}\,K^{-1}} \quad (5)$$

$Zr_{70}Cu_{30}$:

$$C_{p,v} = 27.3 + 1.3 \times 10^{-2}(T - 470)\,\mathrm{J\,mol^{-1}\,K^{-1}} \quad (6)$$

However, the $C_{p,e}$ of $Zr_{67}Cu_{33}$ and $Zr_{70}Cu_{30}$ alloys cannot be determined due to crystallization at a temperature just above T_g.

2. The excess endothermic curves always begin to rise at T_a, regardless of t_a. Furthermore, both the magnitude and the temperature of the endothermic peak tend to increase linearly with the logarithm of the time ($\ln t_a$), as exemplified for $Zr_{70}Cu_{30}$ alloy in Fig. 6.

3. The excess endothermic peak is reversible while the exothermic broad peak is irreversible, and the $C_p(T)$ curve of the annealed samples couples the reversible endothermic and irreversible exothermic reaction.

4. If the annealing is performed at temperatures well below T_g ($T_a \leqslant T_g - 100\,\mathrm{K}$), the glass transition process is not affected. This is indicated by the close overlap of $C_p(T)$ curves for the annealed and as-quenched samples at temperatures below T_g.

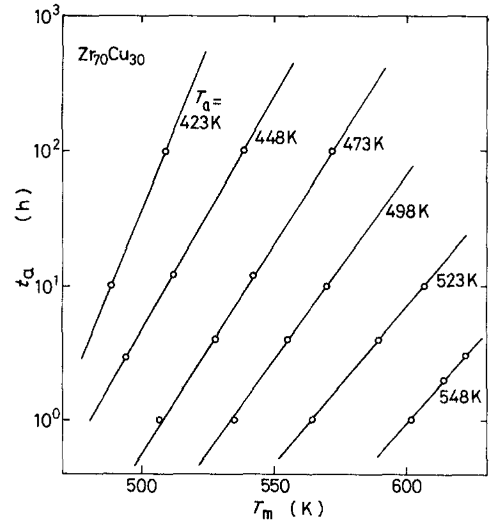

Figure 6 Variation of the $\Delta C_p = C_{p,a} - C_{p,s}$ peak temperature, T_m, as a function of annealing time t_a for an amorphous $Zr_{70}Cu_{30}$ alloy annealed at various temperatures from 423 to 548 K.

3.3. Configuration enthalpy of annealed samples

The change in the configurational enthalpy, $\Delta H_\sigma(T)$, upon annealing at T_a for t_a is evaluated for $Zr_{55}Cu_{45}$ amorphous alloy exhibiting a clear supercooled liquid state and is shown in Figs. 7 and 8. Here the configurational enthalpy of the supercooled liquid at 700 K is taken to be the reference with $\Delta H_\sigma(700\,\mathrm{K}) = 0$, and the relaxed configurational enthalpy $\Delta H_\sigma(T)$ is expressed by

$$\Delta H_\sigma(T) = \int_{700}^{T} (C_{p,a} - C_{p,v})\mathrm{d}T \quad (7)$$

As seen in the figures, the configurational enthalpy curve falls progressively with T_a and t_a, indicating that the low-temperature anneals result in a stabilization of the amorphous structure and a lowering of fictive temperature. With rising temperature, the $\Delta H_\sigma(T)$ of the annealed sample approaches that of the as-quenced sample (not shown) and merges with it before the complete transition from amorphous solid to supercooled liquid, showing that the low-temperature anneals do not affect the relaxation processes near T_g. This feature differs significantly from the previous common phenomenon [11–13] that the $\Delta H_\sigma(T)$ of the amorphous materials annealed in a temperature range slightly below T_g changes significantly even after the glass transition. Additionally, in all cases the $\Delta H_\sigma(T)$ curves cross the equilibrium $\Delta H_{\sigma,e}(T_f = T)$ with

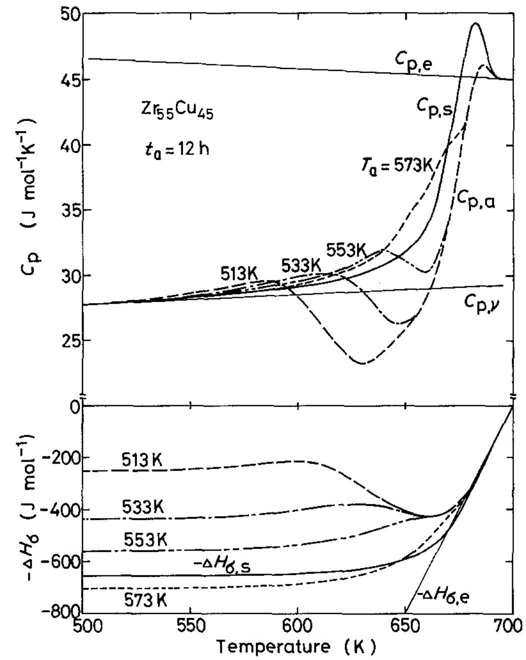

Figure 7 (a) The endothermic peak of an amorphous $Zr_{55}Cu_{45}$ alloy subjected to anneals for 12 h at various temperatures ranging from 513 to 573 K. (b) The change in the configuration enthalpy $\Delta H_\sigma(T)$ corresponding to the appearance of the endothermic peak, where $\Delta H_\sigma(700\,K)$ is set to zero.

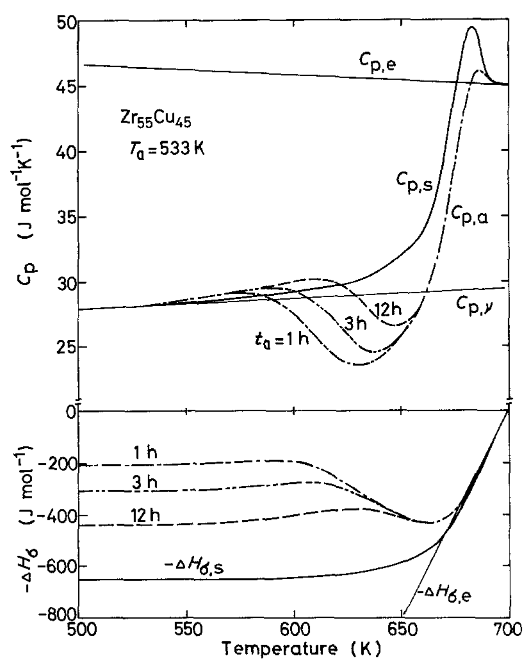

Figure 8 (a) The endothermic peak of an amorphous $Zr_{55}Cu_{45}$ alloy subjected to anneals at 533 K for various periods from 1 to 12 h. (b) The change in the configuration enthalpy $\Delta H_\sigma(T)$ corresponding to the appearance of the endothermic peak, where $\Delta H_\sigma(675\,K)$ is set to zero.

positive slope, and eventually approach equilibrium at high temperature from below the equilibrium curve. The relaxation behaviour, moving away from equilibrium with increasing t_a in the region below T_f is a manifestation of the memory effect and clearly confirms the necessity of a distribution of relaxation times to describe the structural state of the metal–metal type amorphous alloys.

3.4. Changes in $\Delta C_{p,endo}$ with T_a and t_a

The changes in the maximum differential specific heat $\Delta C_{p,max} = C_{p,a} - C_{p,s}$ during annealing for different periods t_a as a function of T_a are shown in Fig. 9 for $Zr_{55}Cu_{45}$, Fig. 10 for $Zr_{67}Cu_{33}$ and Fig. 11 for $Zr_{70}Cu_{30}$. With increasing T_a, the $\Delta C_{p,max}$ of the three alloys increases gradually followed by a rapid increase at temperatures slightly below T_g. The rapid increase in the $\Delta C_{p,max}$ is interpreted to correspond to the common glass transition phenomenon. Fig. 12 shows the change with copper concentration in the maximum values of $\Delta C_{p,endo}$ at the same reduced annealing temperature ($t = T_a/T_g$) of Zr–Cu amorphous alloys during annealing for different periods from 1 to 12 h. In both cases of $t = 0.82$ and 0.89, the $\Delta C_{p,max}$ value decreases with increasing copper content and approaches zero in the vicinity of 50 at % Cu, revealing that the enrichment of copper results in a suppression of the endothermic reaction. Thus, the compositional dependence of the $\Delta C_{p,max}$ varies monotonically and no deflective tendency is seen even at the compositions of deep eutectic and intermetallic compound. Furthermore, it is very

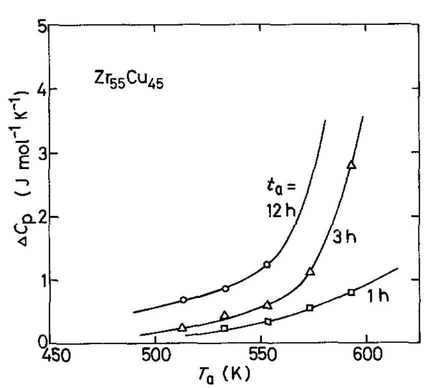

Figure 9 The variation of the maximum differential specific heat $\Delta C_{p,max}$ as a function of annealing temperature T_a, for an amorphous $Zr_{55}Cu_{45}$ alloy subjected to anneals for 1, 3 and 12 h.

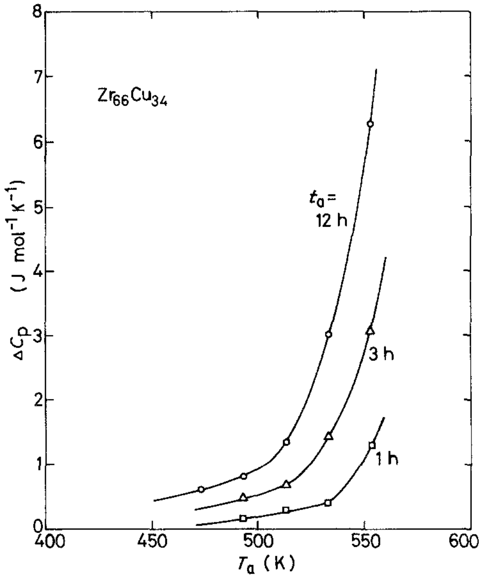

Figure 10 The variation of the maximum differential specific heat $\Delta C_{p,max}$ as a function of annealing temperature T_a, for an amorphous $Zr_{67}Cu_{33}$ alloy subjected to anneals for 1, 3 and 12 h.

important to point out an existence of strong correlation that the lower the Y, H_v, T_g and T_x, the larger is the endothermic enthalpy relaxation. The correlation indicates that the generation of the anneal-induced endothermic relaxation is strongly affected by the bonding force between zirconium and copper atoms.

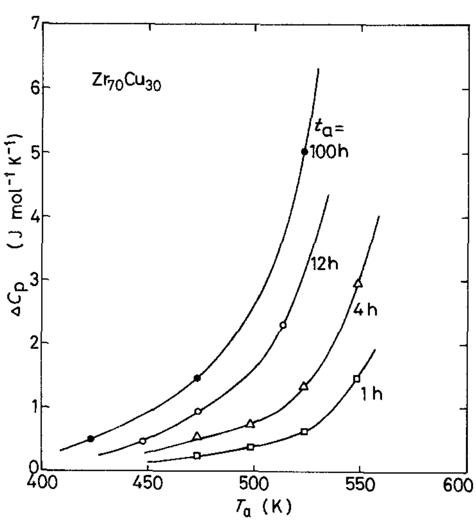

Figure 11 The variation of the maximum differential specific heat $\Delta C_{p,max}$ as a function of annealing temperature T_a, for an amorphous $Zr_{70}Cu_{30}$ alloy subjected to anneals for 1, 10 and 100 h.

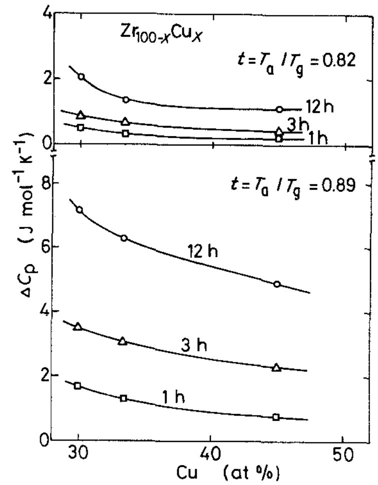

Figure 12 The variation of the maximum differential specific heat $\Delta C_{p,max}$ as a function of copper content for amorphous Zr–Cu alloys subjected to anneals at the same reduced annealing temperatures, $t = T_a/T_g = 0.82$ and 0.89, for 1, 3 and 12 h.

3.5. Effect of third metal elements on $\Delta C_{p,endo,max}(T_a)$ behaviour

The changes in the $\Delta C_{p,max}$ during annealing for 12 h as a function of T_a are shown in Fig. 13 for $Zr_{70}(Cu\text{–}Fe)_{30}$ alloys and in Fig. 14 for $Zr_{70}(Cu\text{–}Ni)_{30}$ alloys, where the data of $Zr_{70}Cu_{30}$ binary alloy are also plotted for comparison. As seen in these figures, the replacement of copper by iron or nickel results in the appearance of an

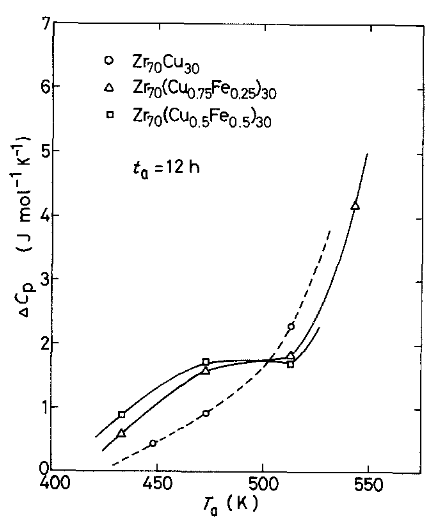

Figure 13 The variation of the maximum differential specific heat $\Delta C_{p,max}$ as a function of annealing temperature for amorphous $Zr_{70}(Cu_{0.75}Fe_{0.25})_{30}$ and $Zr_{70}(Cu_{0.5}Fe_{0.5})_{30}$ alloys subjected to anneals for 12 h. The data for $Zr_{70}Cu_{30}$ alloy are also shown for comparison.

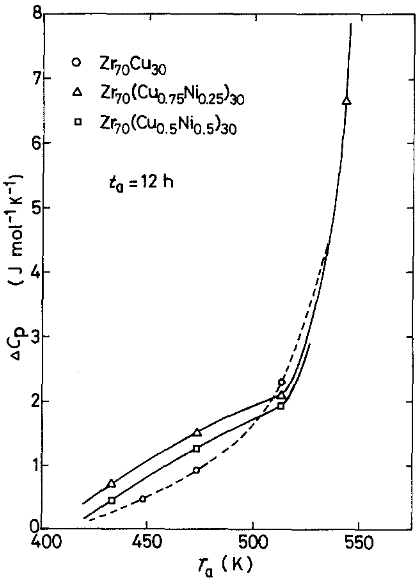

Figure 14 The variation of the maximum differential specific heat $\Delta C_{p,max}$ as a function of annealing temperature for amorphous $Zr_{70}(Cu_{0.75}Ni_{0.25})_{30}$ and $Zr_{70}(Cu_{0.5}Ni_{0.5})_{30}$ alloys subjected to anneals for 12 h. The data for $Zr_{70}Cu_{30}$ alloy are also shown for comparison.

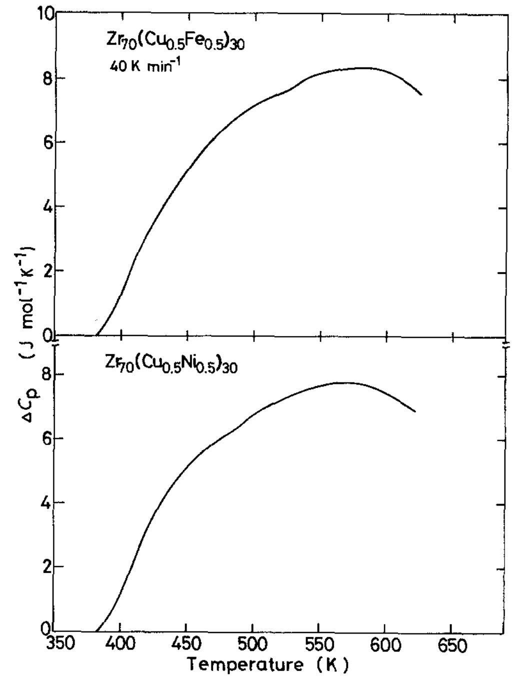

Figure 15 Difference in the specific heat between the as-quenced and annealed states ($\Delta C_{p,exo}$) against temperature for amorphous $Zr_{70}(Cu_{0.5}Fe_{0.5})_{30}$ and $Zr_{70}(Cu_{0.5}Ni_{0.5})_{30}$ alloys.

additional peak at about 475 K in the $\Delta C_{p,max} - T_a$ relation, in addition to the large original peak at about 550 K. Furthermore, it appears important to point out that Zr–Cu–Fe and Zr–Cu–Ni alloys (Fig. 15) also show a two-stage splitting tendency in the temperature dependence of the difference in C_p between the as-quenced and annealed states, $\Delta C_p(T)$, as is seen from a comparison with the data for $Zr_{70}Cu_{30}$ alloy (Fig. 3) showing a single-stage exothermic reaction. From the above-described results, it is clearly concluded that the two-stage splitting of the $\Delta C_{p,endo,max}(T_a)$ and $\Delta C_{p,exo}(T)$ behaviour occurs by the addition of the third metallic elements (iron and nickel), and hence the reason for the appearance of the low-temperature peak originates from the structural relaxation through the interaction among the constituent elements containing iron or nickel. Detailed discussion of this point will be made in Section 4.4.

4. Discussion

4.1. Acitvation energy for enthalpy relaxation $Q_m(T_m)$

The activation energy for structural relaxation can be evaluated from the data of the change of T_m either by isothermal annealing or continuous heating. If the $\Delta C_{p,endo}$ peak at T_m is associated with a single relaxation entity, an apparent activation energy for enthalpy relaxation, Q_m, of Zr–Cu amorphous alloys can be obtained from the isothermal annealing data of Figs. 5 to 8 by using the following relation [14]:

$$\frac{Q_m(T_m)}{k_B} = \frac{d(\ln t_a^*)}{d(1/T_a)} \tag{8}$$

where t_a^* is the annealing time for the appearance of $\Delta C_{p,max}$ at T_m and k_B is Boltzmann's constant. As an example, Fig. 16 shows the log t_a against $1/T_a$ relation for $Zr_{70}Cu_{30}$ amorphous samples. A rather good linear relation, indicating the satisfaction of an Arrhenius temperature dependence, is seen. As plotted in Fig. 17, $Q_m(T_m)$ of the Zr–Cu alloys is not constant and increases with increasing T_m. For instance, the Q_m value of $Zr_{70}Cu_{30}$ alloy increases significantly from 1.4 eV at T_m = 520 K to 4.6 eV at T_m = 620 K.

Alternatively, $Q_m(T_m)$ was evaluated from the shift in the $\Delta C_{p,endo}$ spectrum with scanning rate α from Equation 9 [15, 16] as exemplified in Fig.

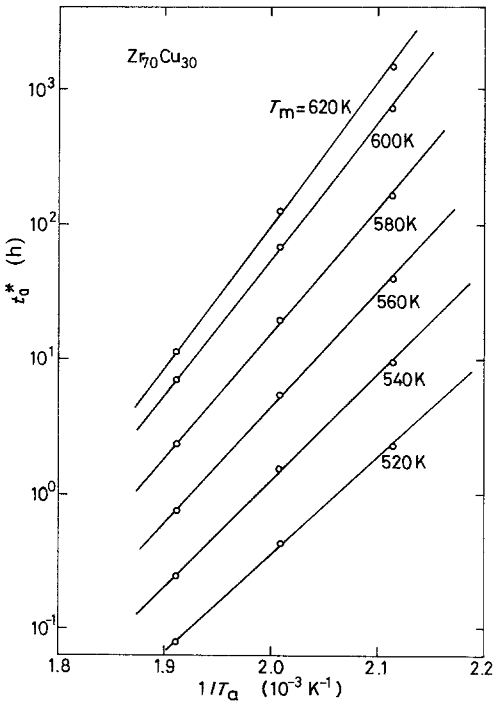

Figure 16 The annealing time t_a^* for the appearance of the ΔC_p peak at T_m as a function of the inverse of the annealing temperature $1/T_a$ for an amorphous $Zr_{70}Cu_{30}$ alloy.

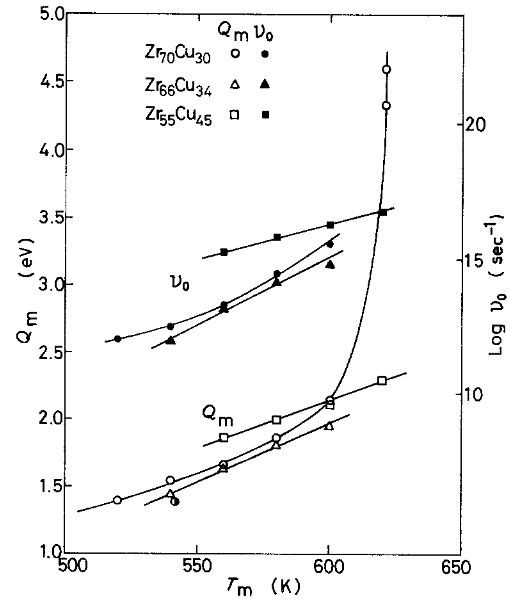

Figure 17 The activation energy spectrum $Q_m(T_m)$, and the frequency factor $\nu_0(T_m)$, as a function of T_m for amorphous $Zr_{55}Cu_{45}$, $Zr_{67}Cu_{33}$ and $Zr_{70}Cu_{30}$ alloys.

18:

$$\frac{Q_m(T_m)}{k_B} \simeq \frac{d[\ln(T_m^2/\alpha)]}{d(1/T_m)} = -2T_m - \frac{d(\ln\alpha)}{d(1/T_m)} \simeq -\frac{d(\ln\alpha)}{d(1/T_m)} \qquad (9)$$

where $T_m \ll Q_m/k_B$. The Q_m values thus evaluated are nearly equal to those obtained from the isothermal data as seen in Fig. 17.

The observed Q_m increases very drastically at temperatures slightly below T_g. The relatively small $Q_m(T_m)$ value in the temperature region of $T_g - 40$ K reflects the occurrence of local and/or medium-range structural relaxation, while the large $Q_m(T_m)$ value at temperatures near T_g is attributed to that of co-operative structural relaxation.

The activation energy Q_m has the following relation to the frequency factor ν_0 and T_m if a first-order reaction process is assumed for the

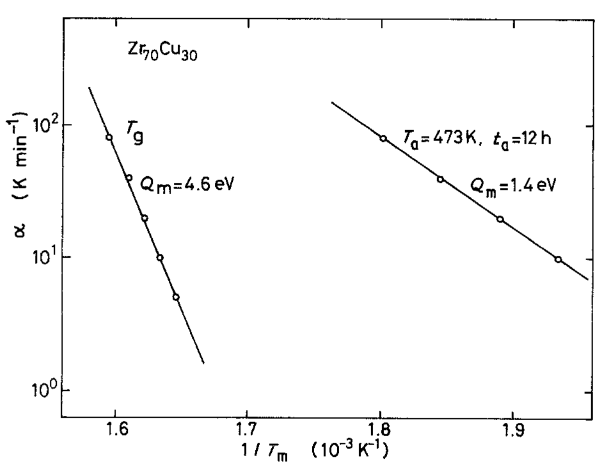

Figure 18 Ozawa plots of $\ln\alpha$ against $1/T_m$ for an amorphous $Zr_{70}Cu_{30}$ alloy.

enthalpy relaxation:

$$\begin{aligned} Q_m &= k_B T_a \ln \nu_0 t_a^* = k_B T_m \ln \nu_0 \tau^* \\ &= Q_m(T_m) \end{aligned} \quad (10)$$

Here τ^* is the relaxation time at T_g and is related to the scanning rate $\alpha = 2/3\,K\,sec^{-1}$ such that $\tau^* = k_B T_m^2/Q_m\,\alpha \simeq 30\,sec$ [17]. The frequency factor $\nu_0(T_m)$ calculated from Equation 10 is plotted in Fig. 17. The ν_0 increases with T_m from $\simeq 10^{15}\,sec^{-1}$ at 560 K to $\simeq 10^{17}\,sec^{-1}$ at 620 K for $Zr_{55}Cu_{45}$, from $\simeq 10^{12}\,sec^{-1}$ at 540 K to $\simeq 10^{15}\,sec^{-1}$ at 600 K for $Zr_{67}Cu_{33}$, and from $\simeq 10^{12}\,sec^{-1}$ at 520 K to $\simeq 10^{16}\,sec^{-1}$ at 600 K for $Zr_{70}Cu_{30}$. These ν_0 values are nearly equal to the Debye frequency $\nu_D \simeq 10^{13}$ to $10^{14}\,sec^{-1}$ in the low-temperature range of $T_g - 40\,K$, and much higher in the higher temperature range. Fig. 17 also shows that both the values of $Q_m(T_m)$ and ν_0 are smaller for the Zr_2Cu compound alloy than for the other two eutectic alloys ($Zr_{55}Cu_{45}$ and $Zr_{70}Cu_{30}$).

4.2. The distribution of the anneal-induced relaxation entity $N_0(T)$

In a previous section, the activation energy for enthalpy relaxation was demonstrated to exhibit a broad distribution against T_m. According to Primak's theory [18] on the kinetics of processes distributed in activation energy, the enthalpy relaxation spectrum as a function of T, $\Delta C_{p,endo}(T)$, is evaluated from

$$\Delta C_{p,endo}(T) = N_0(T)\,\gamma(T) \quad (11)$$

where $N_0(T)$ is the distribution of the relaxation entity, and $\gamma(T)$ is the coupling strength contributing to the specific heat $\Delta C_{p,endo}$. As $\gamma(T) \propto (T - T_a)$ [4]. Equation 11 reduces to

$$N_0(T) \propto \Delta C_{p,endo}(T)/(T - T_a) \quad (12)$$

$N_0(T)$ values of $Zr_{70}Cu_{30}$, $Zr_{70}(Cu_{0.5}Fe_{0.5})_{30}$ and $Zr_{70}(Cu_{0.5}Ni_{0.5})_{30}$ alloys evaluated from the leading edges of $\Delta C_{p,endo}(T)$ are plotted in Fig. 19. It is seen that $N_0(T)$ shows a single maximum near T_g for $Zr_{70}Cu_{30}$ and two separable maxima which peak respectively at about 475 K and T_g for $Zr_{70}(Cu_{0.5}Fe_{0.5})_{30}$ and $Zr_{70}(Cu_{0.5}Ni_{0.5})_{30}$. Thus the $N_0 - T$ curves reproduce fairly well the actually measured distribution of the maximum $\Delta C_{p,endo}$ as a function of T_a shown in Figs. 11, 13 and 14, since $T_m - T_a$ is nearly constant. The

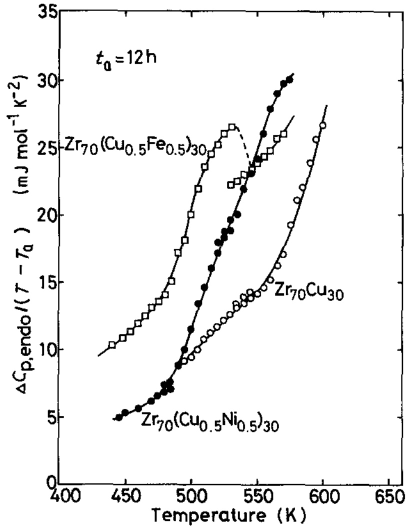

Figure 19 The relaxation entity spectra $N_0(T) = \Delta C_{p,endo}(T)/(T - T_a)$ for amorphous $Zr_{70}Cu_{30}$, $Zr_{70}(Cu_{0.5}Fe_{0.5})_{30}$ and $Zr_{70}(Cu_{0.5}Ni_{0.5})_{30}$ alloys as a function of temperature.

good reproducibility enables us to conclude clearly that the relaxation entity distributes over one stage against T_a and t_a for $Zr_{70}Cu_{30}$ alloy and over two stages for $Zr_{70}(Cu_{0.5}Fe_{0.5})_{30}$ and $Zr_{70}(Cu_{0.5}Ni_{0.5})_{30}$ alloys. Judging from the result that the T_a dependence of $\gamma(T)$ and the relatively large frequency factor $\nu_0 > \nu_D$ are similar to the relaxation behaviour commonly observed for anneal at temperatures just below T_g, the single-stage relaxation spectrum for the Zr–Cu alloy is therefore thought to be attributed to a distribution of one kind of glass transition (T_g) with an apparent activation energy Q_m. Similarly, each spectrum of the first- and second-stage relaxations for the Zr–Cu–Fe and Zr–Cu–Ni alloys is attributed phenomenologically to a distribution of two kinds of characteristic glass transitions (T_{g1} and T_{g2}) with an individual apparent activation energy Q_1 and Q_2.

4.3. Interpretation of the single-stage endothermic reaction of Zr–Cu binary alloys

It has recently been proposed [4, 19, 20] that a supercooled liquid structure near T_g is inhomogeneous and consists of liquid-like regions of large free volume or high local free energy, and solid-like regions with small free volume or low local free energy. The resulting amorphous solid prepared by melt-quenching contains a large number of liquid-like regions with unrelaxed atomic configuration which are isolated from each other and embedded in the solid-like matrix. The inhomogeneity in the Zr–Cu amorphous alloys is thought to arise from fluctuations in concentration and density. When the amorphous solid is annealed at T_a for t_a, parts of the liquid-like regions undergo configurational changes to a more relaxed state in an independent and non-co-operative manner. However, the local structural relaxation in a cluster involving several atoms can be co-operative, and the size of this cluster has been estimated to be less than 1–2 nm. Each liquid-like region, m, manifests a liquid–amorphous transition at $T_{g,m}$ which depends on its atomic configuration state. When an amorphous alloy is annealed at temperatures well below T_g, the regions with characteristic relaxation times τ_m given by Equation 13 below, being shorter than the duration of the annealing time t_a, where $\tau_m < t_a$, undergo local relaxation towards the local equilibrium states at T_a:

$$\tau_m \simeq \tau_{mea} \exp\left[-\frac{Q_m}{k_B}\left(\frac{1}{T_a} - \frac{1}{T_{g,m}}\right)\right] \quad (13)$$

Here, τ_{mea} is the time constant of measurements. Each local relaxation contributes to the enthalpy relaxation in proportion to $(T_a - T_{g,m})$. Upon heating the annealed sample, each region, m, recovers the initial structure (the so-called "reversion") and contributes to an excess endothermic specific heat as the local amorphous–liquid transition occurs at or slightly above $T_{g,m}$. Thus the peak temperature of the $\Delta C_{p,endo}$ evolves in a continuous manner against the logarithm of t_a with intensity proportional to $(T_{g,m} - T_a)N_0(T_{g,m})$. Therefore, the reason why the endothermic reaction for the Zr–Cu binary amorphous alloys evolves over a single stage is concluded to be due to a monotonic increase of $N_0(T_{g,m})$ for the binary amorphous alloys as a function of temperature.

4.4. Interpretation of the two-stage endothermic reaction of Zr–Cu–Fe and Zr–Cu–Ni alloys

Although the above-described concept gives reasonably a single broad distribution of relaxation times (or glass transitions), it does not give an interpretation of the appearance of the two-stage endothermic peaks. Most recently, Inoue *et al.* [7] have found that the metal–metalloid amorphous alloys containing more than two kinds of metal elements such as (Fe, Co, Ni)–Si–B, Fe–Ni–P and Fe–Ni–B systems annealed at temperatures below T_g exhibit two distinctly distinguishable endothermic peaks, and the appearance of the two peaks has been interpreted on the new concept of a two-stage distribution of relaxation times (or glass transitions) centring at T_{g1} and T_{g2}. Here T_{g1} corresponds to the glass transition arising from metal atoms (iron, nickel and cobalt) with a weak bonding nature, and T_{g2} to that from metal–metalloid atoms with a strong bonding nature. The reason for the appearance of the two-stage endothermic peak which was found for the first time for the metal–metal type Zr–Cu–Fe and Zr–Cu–Ni amorphous alloys can be reasonably explained by the same mechanism. In the Zr–Cu–Fe and Zr–Cu–Ni ternary systems, the metallic bonding force between zirconium and copper, iron or nickel is thought to be much stronger than that between copper and iron or nickel, as is evidenced from the fact that an amorphous phase is easily formed in Zr–Cu, Zr–Fe and Zr–Ni alloys while no amorphous phase is obtained in Cu–Fe and Cu–Ni alloys. Therefore, the Cu–Fe and Cu–Ni pairs are more or less confined to the skeleton of Zr–Cu and Zr–Fe or Zr–Ni pairs. The local-range rearrangement of copper and iron or nickel atoms with a weak bonding occurs in the low-temperature range, while the atomic regroupings involving zirconium and copper (iron or nickel) atoms take place co-operatively at higher temperatures near T_g because of the limitation of atomic rearrangement due to their strong bonding nature. It is thus concluded that the marked difference in bonding force among the constituent elements is a main reason for an appearance of the two-stage enthalpy relaxation which is evidenced from the data (Fig. 19) showing a two-stage distribution of the $N_0(T)$ curve of the Zr–Cu–Fe and Zr–Cu–Ni amorphous alloys. In addition, the reason why the magnitude of the endothermic peak for Zr–Cu amorphous alloys reduces with increasing copper content is thought to originate from an enhancement of the difficulty in atomic rearrangement during annealing (an increase in relaxation times) due to the increase in the number of Cu–Zr pairs with a strong bonding force and the decrease in that of Zr–Zr pairs with a weak bonding force. Thus, the effect of copper on the enthalpy relaxation behaviour as well as Y, H_v, T_g and T_x of Zr–Cu amorphous alloys is concluded to be quite similar to that [5, 21] of metalloid elements for metal–metalloid type amorphous alloys.

5. Summary

In order to clarify the anneal-induced relaxation behaviour of a metal–metal type amorphous alloy structural relaxation of $Zr_{50}Cu_{50}$, $Zr_{55}Cu_{45}$, $Zr_{67}Cu_{33}$ and $Zr_{70}Cu_{30}$ binary and $Zr_{70}(Cu_{1-x}Fe_x)_{30}$ and $Zr_{70}(Cu_{1-x}Ni_x)_{30}$ ternary amorphous alloys has been investigated calorimetrically for samples annealed over a wide temperature range from well below T_g to T_g. The results obtained are summarized as follows:

1. Upon heating the annealed samples, an excess endothermic reaction (enthalpy relaxation) occurs above T_a followed by a broad exothermic reaction. The peak temperature of the endothermic specific heat $\Delta C_{p,endo}$, T_m, increases in a continuous manner with $\ln t_a$.

2. The magnitude of $\Delta C_{p,endo}$ decreases with increasing copper content, and no endothermic reaction is seen in $Zr_{50}Cu_{50}$ alloy even at $T_a \simeq T_g$. There is a clear tendency that the lower the hardness and the Young's modulus, the larger is the $\Delta C_{p,endo}$ peak.

3. The change in the magnitude of the $\Delta C_{p,endo}$ peak with T_a for Zr–Cu binary alloys occurs at a single stage with a peak at $\simeq T_g$. On the other hand, that for the Zr–Cu–Fe and Zr–Cu–Ni ternary alloys can be separated into two stages: a low-temperature (first-stage) peak at about $T_g - 150\,K$ and a high-temperature (second-stage) peak at a temperature slightly below T_g. The activation energy for the enthalpy relaxation of Zr–Cu binary alloys increases with increasing T_m from $\simeq 1.4\,eV$ at $T_m \simeq 0.85\,T_g$ to $\simeq 4.5\,eV$ at $T_m \simeq T_g$.

4. From the result that the addition of iron or nickel results in the appearance of another low-temperature peak in the $\Delta C_{p,endo}$–T_a relation, the endothermic reaction was interpreted as due to local and medium-range rearrangements of Cu–Fe or Cu–Ni atoms with a weak bonding nature for the first-stage peak and to the long-range co-operative rearrangements of Zr–Cu, Zr–Fe and Zr–Ni atoms, which are composed of the skeleton structure in Zr–Cu type amorphous alloys, for the second-stage peak. By the endothermic reaction each region recovers from the relaxed configuration caused by annealing to an unrelaxed initial structure. The occurrence of the two-stage reversible enthalpy relaxation for the Zr–Cu–Fe and Zr–Cu–Ni alloys appears to originate from a dual distribution of glass transitions centred around T_{g1} and T_{g2}, which arise respectively from copper and iron or nickel atoms and from zirconium and copper, iron or nickel atoms.

References

1. H. S. CHEN, *J. Appl. Phys.* **52** (1981) 1868.
2. *Idem*, Proceedings of the 4th International Conference on Rapidly Quenched Metals, Sendai, Japan, August 1981, edited by T. Masumoto and K. Suzuki (Japan Institute of Metals, Sendai, 1982) p. 495.
3. J. W. DRIJVER, A. L. MULDER and S. RADELAAR, *ibid.*, p. 535.
4. H. S. CHEN, *J. Non-Cryst. Solids* **46** (1981) 289.
5. H. S. CHEN and A. INOUE, *ibid.* **61/62** (1984) 805.
6. A. INOUE, T. MASUMOTO and H. S. CHEN, *J. Mater. Sci.* **19** (1984) 3953.
7. *Idem, ibid.* **20** (1985) in press.
8. M. HARMELIN, Y. CAVAYRAC, A. QUIVY, J. BIGOT, P. BURNIER and M. FAYARD, *J. Non-Cryst. Solids* **61/62** (1984) 931.
9. F. SOMMER, H. HAAS and B. PREDEL, *ibid.* **61/62** (1984) 793.
10. H. S. CHEN and J. T. KRAUSE, *Scripta Metall.* **11** (1977) 761.
11. A. J. KAVACS, *Fotchr. Hochpolym – Forsch* **3** (1963) 394.
12. H. S. CHEN, *J. Appl. Phys* **49** (1978) 4595.
13. R. O. SUZUKI and P. H. SHINGU, *J. Non-Cryst. Solids* **61/62** (1984) 1003.
14. H. S. CHEN, *ibid.* **27** (1978) 257.
15. T. OZAWA, *Polymer* **12** (1971) 51.
16. C. ANTONIONE, L. BATTEZZATI, A. LUCCI, G. RIONTINO and G. VENTURELLO, *Scripta Metall.* **12** (1978) 1011.
17. H. S. CHEN, *Sci. Rep. Res. Inst. Tohoku Univ.* **A-27** (1979) 97.
18. W. PRIMAK, *Phys. Rev.* **100** (1955) 1677.
19. M. H. COHEN and G. S. CREST, *ibid.* **B20** (1979) 1077.
20. M. CYAT, *J. Phys.* **C8** (1980) 107.
21. A. INOUE, T. MASUMOTO and H. S. CHEN, unpublished research (1984).

Received 23 November
and accepted 19 December 1984